

Accepted Manuscript

Monitoring of particle motions in gas-solid fluidized beds by electrostatic sensors

Yao Yang, Qing Zhang, Can Zi, Zhengliang Huang, Wenbiao Zhang, Zuwei Liao, Jingdai Wang, Yongrong Yang, Yong Yan, Guodong Han

PII: S0032-5910(16)30818-X
DOI: doi:[10.1016/j.powtec.2016.11.034](https://doi.org/10.1016/j.powtec.2016.11.034)
Reference: PTEC 12110

To appear in: *Powder Technology*

Received date: 22 June 2016
Revised date: 6 November 2016
Accepted date: 23 November 2016



Please cite this article as: Yao Yang, Qing Zhang, Can Zi, Zhengliang Huang, Wenbiao Zhang, Zuwei Liao, Jingdai Wang, Yongrong Yang, Yong Yan, Guodong Han, Monitoring of particle motions in gas-solid fluidized beds by electrostatic sensors, *Powder Technology* (2016), doi:[10.1016/j.powtec.2016.11.034](https://doi.org/10.1016/j.powtec.2016.11.034)

This is a PDF file of an unedited manuscript that has been accepted for publication. As a service to our customers we are providing this early version of the manuscript. The manuscript will undergo copyediting, typesetting, and review of the resulting proof before it is published in its final form. Please note that during the production process errors may be discovered which could affect the content, and all legal disclaimers that apply to the journal pertain.

Monitoring of particle motions in gas-solid fluidized beds by electrostatic sensors

Yao Yang¹, Qing Zhang¹, Can Zi¹, Zhengliang Huang¹, Wenbiao Zhang², Zuwei Liao¹, Jingdai Wang^{1*}, Yongrong Yang¹, Yong Yan^{2,3}, Guodong Han⁴

¹ State Key Laboratory of Chemical Engineering, College of Chemical and Biological Engineering, Zhejiang University, Hangzhou, 310027, China

² School of Control and Computer Engineering, North China Electric Power University, Beijing, 102206, China

³ School of Engineering and Digital Arts, University of Kent, Canterbury, Kent CT2 7NT, U.K.

⁴ Tianjin Branch Company of SINOPEC, Tianjin, 300271, China

*Corresponding Author. Tel: +86-571-87951227; Fax: +86-571-87951227.

Email: wangjd@zju.edu.cn

Abstract

Gas-solid fluidized beds are widely applied in numerous industrial processes. Particle motions significantly affect the performance of fluidized bed reactors and the characterization of particle movements is therefore important for fluidization quality monitoring and scale-up of reactors. Electrostatic charge signals in the fluidized bed contain much dynamic information on particle motions, which are poorly understood and explored. In this work, correlation velocities of Geldart B and D particles were measured, analyzed and compared by induced electrostatic sensors combined with cross-correlation method in the fluidized bed. The results indicated that the average correlation velocity of particle clouds increased and the normalized probability density distributions of correlation velocities broadened when the superficial gas velocity increased in the dense-phase region. Both upward and downward correlation velocities could be acquired in the dynamic bed level region. Under the same excess gas velocity, the average correlation velocity of Geldart D particles was significantly smaller than that of Geldart B particles, which was caused by the smaller bubble sizes caused by the dominant bubble split over coalescence and less volume of

gas forming bubbles for Geldart D particles. The experimental results verified the reliability and repeatability of particle correlation velocity measurement by induced electrostatic sensors in the gas-solid fluidized bed, which provides definite potential in monitoring of particle motions.

Key words:

Induced electrostatic signal; gas-solid fluidized bed; cross-correlation method; correlation velocity

1. Introduction

Gas-solid fluidized beds are widely applied in numerous industrial processes, such as coal combustion and gasification, granulation and drying, olefin polymerization, etc. The bubble-induced solids circulation within the bed leads to good contact and mixing of gas and solid phases, and high rates of heat transfer [1]. Electrostatic charge generation and accumulation on insulated particles are almost unavoidable due to repeated particle-particle and particle-wall frictions in the gas-solid fluidized bed. An excess accumulation of electrostatic charges will cause problems such as wall sheeting [2], particle agglomeration [3, 4], and even spark generation or explosion hazards [5-7]. The generation and variation of electrostatic charge signals are significantly affected by bubble and particle motions inside the fluidized bed, which contain much dynamic information related to hydrodynamic behaviors. However, the hydrodynamic information contained in electrostatic charge signals is poorly understood and needs more comprehensive analysis [8, 9].

Considerable efforts have been made to investigate the relations between electrostatic charge signals and hydrodynamic behaviors in the gas-solid fluidized bed [10-14]. However, interpretation and decoupling of electrostatic signals to reveal bubble behaviors or particle motions are relatively limited. Zhang et al. [15] compared the similarity between electrostatic current and pressure drop in a specific fluidized bed and proposed a quantitative relation between these two signals, which provided the possibility to utilize electrostatic current to characterize bubble behaviors. He et al. [9, 16-18] designed novel electrostatic probes to simultaneously measure the particle charge density and bubble properties, whose results were in good agreement with those from Faraday cup sampling system and video images, respectively. The aforementioned research focused on decoupling the electrostatic signals to reveal bubble behaviors in the fluidized bed. However, characterization of particle motions by electrostatic probes is rarely reported in the

gas-solid fluidized bed, but mostly applied in dilute gas-solid systems. Extensive work has been carried out to measure particle motions by cross correlating electrostatic signals derived from a pair of axially spaced electrostatic sensors installed on the outer wall of pneumatic conveying pipes. Yan et al. [19] conducted theoretical and experimental studies of the cross-correlation technique applied to the velocity measurement of pneumatically conveyed solids using ring-shaped electrostatic sensors. The repeatability of this method was demonstrated in both bench-scale and pilot-plant trials. Zhang et al. [20] set ring-shape and arc-shape electrostatic sensors in the riser and downer of the circulating fluidized bed and found that both the particle correlation velocity and the standard deviation (STD) of electrostatic signals increased with superficial gas velocity. Xu et al. [21, 22] measured the mean velocity of solid particles in both dilute and dense-phase pneumatic conveying pipes based on spatial filtering effect of the electrostatic sensor and cross-correlation method, respectively. The relative error in the dense-phase system was obviously larger than that in the dilute pipe because the particle concentration profile fluctuated continuously due to the instability of the dense-phase gas-solid flow [23]. Although electrostatic sensors combined with cross-correlation method have been widely investigated or even applied to monitor particle motions in dilute gas-solid systems, scarcely any research about the application of this method in gas-solid fluidized beds has been reported.

Particle motions and flow patterns significantly affect the performance of fluidized bed reactors (FBRs), therefore, the characterization of solids motion and mixing is essential for the monitoring of fluidization quality, proper design and scale-up of FBRs [24]. Several experimental techniques have been developed to measure and analyze particle motions in the gas-solid fluidized bed. Parker et al.[25] applied positron emission particle tracking (PEPT) to obtain the particle moving trajectories, particle velocity and circulation pattern within the bed, which has been successfully applied in bench-scale fluidized beds, wurster fluidized beds [26] and rotating drums [27]. Mostoufi et al.[28] measured the axial and radial diffusion coefficients of particles in the fluidized bed by radioactive particle tracking (RPT) technique. The results showed that the diffusivities increased with superficial gas velocity and were linearly correlated to the axial solid velocity gradient. Particle image velocimetry (PIV) is mostly used for the measurement of particle velocity profiles around the bubble [29] and in the emulsion phase, bubble size and rise velocity

[30] in two-dimensional fluidized beds. Laser Doppler velocimetry (LDV) can be employed to simultaneously obtain the velocity profiles of both gas and solid phases [31, 32]. By inserting the optical fiber probes [33, 34] into the fluidized bed, the received light reflected by moving particles is converted into voltage signals. The solids concentration can be obtained by calibrating the relationship between the output signals and the solids volume concentration, and the two sub-probes enable to measure the instantaneous local particle velocity with cross-correlation method [34]. Acoustic emission (AE) method has been applied to monitor the particle fluidization pattern and the activity of particle motions in the fluidized bed [35, 36]. Considering of the unique intrinsic characteristics and data processing methodologies associated with each of the above measurement techniques, each technique has its own limitations in its application. For example, radioactive tracer particles need to be added to the measured system in the PEPT and RPT techniques. Therefore, the moving trajectories and velocities which come from a single particle cannot show entirely the movement intensity and direction of local bulk particles. Due to the existence of light source, PIV and LDV methods can only be applied to transparent fluidized beds, or fluidized beds with glass windows. Besides, velocity measurement can be carried out only on the front-layer particles [37] for LDV method. The optical fiber probe is intrusive, and therefore interferes to some extent with the flow field being measured. Furthermore, electrostatic and van de Waals forces may cause fine particles to adhere to the optical probe surface, leading to significant loss of data [38]. Moreover, for the measurement of solids volume concentrations, the calibration process is quite difficult since it is practically impossible to realize homogeneous gas-solid suspension [39]. AE method could recognize the circulation pattern of particles but could not give the specific velocities and directions of particle motions. In dilute gas-solid flow systems, since the electrostatic signals detected are affected by all the moving charged particles in the sensitivity zone of the sensor, the correlation velocity represents the average velocity of a certain number of particles [19]. Therefore, compared with the instantaneous or local velocity measured by the methods mentioned above, correlation velocity is more macroscopic, which could reflect the intensity of particle motions as well and provide supplementary information on particle movements.

In comparison with dilute gas-solid systems, particle motions in the fluidized bed are more complicated and distributions of particle velocity and concentration are more distinct, but the

mechanisms of electrostatic charges induction on the electrostatic sensors are almost the same. Therefore, the application of cross-correlation method to the electrostatic charge signals measured in the fluidized bed could provide a new way to characterize particle motions.

To demonstrate the feasibility of this method applied in the gas-solid fluidized bed, verification of the correlation between electrostatic signals detected and the reliability of particle correlation velocity are imperative. This work was to measure the correlation velocities of Geldart B and D particles by induced electrostatic sensors combined with cross-correlation method in the gas-solid fluidized bed. The average correlation velocity of particles was compared with the superficial gas velocity and the theoretical bubble rise velocity to explore the reliability of this method to monitor particle motions. Based on the experimental results of correlation velocity measurement for particles of different Geldart types, the movement and fluidization characteristics of Geldart B and D particles were analyzed and compared.

2. Experimental apparatus and materials

Fig. 1 shows the schematic diagram of the experimental apparatus, which consists of fluidization system and measurement system. The fluidized bed is made of a transparent Plexiglas column with an inner diameter of 140 mm and a height of 1000 mm. The thickness of the Plexiglas column is 5 mm. The expanded section at the top has a height of 300 mm and a width of 250 mm. An iron perforated distributor is installed at the bottom of the column with 226 holes and an open area ratio 2.6%, along with a gas mixing chamber. Compressed air pre-dried to a relative humidity of 8-15% and within the temperature range of 20-25 °C is used as the fluidizing gas.

The measurement system is composed of electrostatic sensors, electrostatic signal amplification circuits, a data acquisition card (National Instruments, USB-6212) and a computer. Considering the fact that the signal measured by ring-shape electrostatic sensors is the average value of the entire cross-section while distributions of particle velocity and concentration in the same cross-section might be more distinct in the fluidized beds, the arc-shaped electrostatic sensors were used in this work to measure the differences among different directions of the cross-section. Sensors are made of copper with a width of 6 mm and a thickness of 2 mm. The central angle of the sensor is 60 degree. The arc-shaped electrodes were tightly wrapped on the outer wall of the fluidized bed, with four electrodes at the same level. The installation layout of

electrostatic sensors is shown in Fig. 2. In each set of the electrodes, the distance between the two adjacent electrodes was 25 mm. The electrodes were numbered 1 to 12 from the distributor to the top, respectively. S 1-2 will be used below to represent the correlation velocity obtained by electrostatic signals from sensors 1 and 2, and by this analogy.

When charged particles come across the sensitivity zone of electrodes, induced electrostatic charges on the electrodes are affected and electrostatic current is generated, which is transformed, filtered and amplified to electrostatic voltage signal by signal amplification circuit. Grounded metal boxes were installed outside the electrodes and circuit boards in order to eliminate external electrical interference and enhance the signal-to-noise ratio. Electrostatic voltage signals from all the electrodes were recorded in a computer through the data acquisition card. The sampling time period was 200 s. The selection of the sampling frequency was determined by the measurement error, the measuring range of velocity and the space between adjacent electrostatic sensors [40], which would be discussed in Section 3.2.

The fluidized particles used in the experiment were linear low density polyethylene (LLDPE) particles and polypropylene (PP) particles, supplied by a branch company of SINOPEC. Specific physical properties of the particles and operating parameters are indicated in Table 1. The minimum fluidization velocity (u_{mf}) was determined by the conventional pressure drop method. The fluidized bed was operated in the bubbling flow regime in the superficial gas velocity (u) range covered in these experiments. The static height of the bed was kept at 265 mm when different types of particles were used.

3. Cross-correlation method and parameter selection

3.1. Characteristics of induced electrostatic signals in time and frequency domains

When particles were charged to a saturate level after fluidization for over 30 min, induced electrostatic voltage signals on the electrostatic sensors were recorded simultaneously for 200 s. Fig. 3(a) shows the induced electrostatic voltage signals from the upstream ($H=205$ mm, S 4) and downstream ($H=230$ mm, S 5) electrostatic sensors during fluidization process at a superficial gas velocity of 0.5 m/s. It can be seen that the fluctuations of electrostatic voltage were similar between the upstream and downstream signals, while there existed a time difference between the

signals sequences. The time difference was denoted as τ in the Fig. 3(a). The corresponding power spectral density (PSD) of electrostatic voltage is displayed in Fig. 3(b). It was demonstrated that in the dense-phase pneumatic conveying system, the energy of the electrostatic fluctuation was mainly distributed in the frequency range of 0-300 Hz, and the peak frequency moved toward higher frequency with increasing superficial gas velocity [41]. Compared with the pneumatic conveying system, the PSDs of electrostatic voltage signals in the gas-solid fluidized bed were mainly located between 0-5 Hz. The difference of frequency distributions in PSDs is caused by the difference of superficial gas velocity, or solid velocity in these two systems. The particle velocity in the pneumatic conveying system is always 1-2 magnitude orders larger than that in the gas-solid fluidized bed. Due to the difference of intrinsic characteristics of signals from various gas-solid systems, some parameters should be carefully selected first before calculating the correlation velocity.

3.2. Selection of parameters for cross-correlation calculation

The cross-correlation coefficient $R_{xy}(\tau)$ of electrostatic signals between the upstream and downstream electrodes can be calculated by the following Eq. [40]:

$$R_{xy}(\tau) = \frac{1}{T} \int_0^T y(t) x(t - \tau) dt \quad (1)$$

where $x(t)$ and $y(t)$ represent the upstream and downstream electrostatic signals, respectively. T is the integral time. The corresponding time lag of maximum correlation coefficient is the time difference between the upstream and downstream signals, which is also called transit time (τ_m). Then the particle correlation velocity can be obtained by Eq. (2),

$$v_c = \frac{L}{\tau_m} \quad (2)$$

in which L is the distance between the centers of adjacent electrostatic sensors, which was 25 mm in this work. In the gas-solid pipeline flow system, the meter factor, K , is always introduced to express the relationship between the mean particle velocity (v_m) and the correlation velocity (v_c) [19]. The relative magnitude of the mean particle velocity can be reflected by the value of the correlation velocity.

The cross-correlation function of the electrostatic voltage signals shown in Fig. 3(a) is

revealed in Fig. 4. An obvious peak value of cross-correlation coefficients can be found and the peak value reflects the similarity between the upstream and downstream signals. When the maximum correlation coefficient exceeds 0.6, it means that the upstream and downstream signals are remarkably correlated, which is the basis of the following calculation.

Selection of sampling frequency

The selection of sampling frequency is strongly influenced by the characteristics of the electrostatic signal. Zhang et al. pointed out that the sampling frequency (f) should be

$$f \geq \frac{100v_{\max}}{2\delta L}, \quad (3)$$

where L is the distance between adjacent electrostatic sensors, δ represents the tolerance of the standard deviation of the transit time, and v_{\max} is the maximum velocity in the measuring process, which could be estimated by the bubble rise velocity in the fluidized bed. The upward velocity of the particles in a wake of a bubble should be equal to the bubble rise velocity [42], and greater than the velocities of particles in other parts of the fluidized bed. Therefore, the bubble rise velocity was calculated to estimate the maximum particle velocity in the fluidized bed.

The theoretical Eq. for bubble rise velocity calculation is shown in Eq. (4) [43].

$$u_b = (u - u_{mf}) + 0.711(gd_b)^{1/2} \quad (4)$$

In Eq. (4), u_b is the bubble rise velocity and d_b is the bubble diameter, which is calculated by the following Eq. (5) proposed by Mori and Wen [44],

$$\frac{d_{bm} - d_b}{d_{bm} - d_{b0}} = e^{-0.3z/d_t} \quad (5)$$

$$d_{bm} = 0.652 \left[\frac{\pi}{4} d_t^2 (u - u_{mf}) \right]^{0.4} \quad (6)$$

$$d_{b0} = 0.347 \left[\frac{\pi}{4} d_t^2 (u - u_{mf}) / N_0 \right]^{0.4} \quad (7)$$

where d_t is the inner diameter of the fluidized bed and d_{b0} is the initial bubble diameter formed at the surface of the perforated distributor. N_0 is the number of holes in the distributor. In this work, the maximum z was 0.6 m, therefore, the corresponding bubble rise velocity was 1.22 m/s. The tolerance of the standard deviation of the transit time was set to be $\pm\delta\% = \pm 2\%$. The sampling frequency could be calculated by Eq. (3) as follows:

$$f \geq \frac{100 \times 1.22}{2 \times 2 \times 0.025} = 1220 \text{ Hz} \quad (8)$$

Considering that the particle motions in the fluidized bed are so complicated that the velocity of particles may be greater than the theoretical bubble rise velocity due to the collisions between particles, the sampling frequency was selected as 4000 Hz in this work. The sampling time was 200 s.

Selection of integral time

The integral time, T , represents the number of data points used in the cross-correlation calculation. The longer the integral time is, the more accurate the correlation result should be. However, the increase in the integral time will decrease the dynamic response of the system and require higher level hardware performance to calculate the correlation function [40]. It was found that when the integral time is short, the standard deviation (STD) of correlation velocity will increase as the integral time gets longer. If the integral time reaches a certain value, the STD will not change obviously with the increase of integral time. Fig. 5 shows the variation of STD with the integral time. It can be indicated that when the integral time reached 2 s, the value of STD became relatively stable with the integral time increasing.

According to the cross-correlation principle [45], the integral time should also satisfy the following relationship,

$$T \geq 10\tau_0 \quad (9)$$

where τ_0 is the first zero crossing point in the auto-correlation function of electrostatic signals. The maximum τ_0 was 0.15 s in this experiment, which meant that T should be greater than 1.5 s. Compared with the result obtained in the STD calculation process, the integral time in this work was selected as 2 s. Since the sampling time was 200 s, 100 correlation velocity values can be obtained from two adjacent electrostatic sensors, but not all the calculated values are valid. The correlation velocity will be discarded if the maximum correlation coefficient is less than 0.6 [20, 33].

4. Results and discussions

4.1. Characterization of Geldart B particle motions by electrostatic sensors

Induced electrostatic voltage signals were detected when charged particles approached or left

the sensitivity zone of electrostatic sensors in the gas-solid fluidized bed. Since all the particles in the sensitivity zone contributed to the generation and variation of electrostatic voltage, the correlation velocity obtained by cross-correlating the upstream and downstream signals was regarded as the correlation velocity of the particle cloud in the sensitivity zone in this work, which could reflect the movement intensity of a number of charged particles. The minimum dynamic bed level was 330 mm during the experiment and the dynamic bed level range was 330-590 mm. Therefore, in the discussions below, the region covered by sensors S 1-7 is called the dense-phase region of the fluidized bed, and the region covered by S 8-12 is called the dynamic bed level region.

Fig. 6 indicates the 100 correlation coefficients calculated from the signals shown in Fig. 3(a) and the corresponding correlation velocities. As shown in Fig. 6(a), the maximum correlation coefficients were in the range of 0.6-1 when the integral time was 2 s. The ratio of the maximum coefficients greater than 0.6 was over 90% for different trials with various superficial gas velocities in the fluidized bed of Geldart B particles, which means that the upstream and downstream electrostatic signals in the gas-solid fluidized bed showed a remarkable correlation under different superficial gas velocities. This was the precondition of this method used in the dense gas-solid flow system. Fig. 6(b) displayed the correlation velocities calculated by the transit time corresponding to each maximum correlation coefficient. It can be seen that the correlation velocity fluctuated in the range of 0.3-0.7 m/s with relative errors no more than 18.1%. The charged particle cloud might locate in the wake or the drift of the bubble, or in the emulsion phase when it passed through the sensitivity zone of the electrostatic sensors [24], and consequently, the velocities of particle clouds were intrinsically different during the measurement. Besides, the mutual disturbance and coalescence of bubbles would also affect the velocity of particle clouds. Consequently, the correlation velocity measured was not a fixed value, but fluctuated within a certain range.

Fig. 7 showed the normalized probability density distributions of correlation velocities measured by the same sensors pair as in Fig. 6 under different superficial gas velocities. As the superficial gas velocity increased, the distribution of correlation velocities broadened and the correlation velocity corresponding to the peak became greater, which means that the motions of charged particle clouds became more vigorous with the increase of gas velocity. The average

correlation velocity of particle clouds, which was the average of all the valid correlation velocities as shown in Fig. 6(b), was used to represent and compare the magnitude of particle velocity below.

Fig. 8 indicated the average correlation velocities of particle clouds measured by sensor pairs S 1-2 and S 4-5, which were both in the dense-phase region, with the error bars representing STDs of the correlation velocities. It can be seen that with the increase of superficial gas velocity, the average correlation velocity of particle clouds increased in the dense-phase region of the fluidized bed. The average correlation velocity was greater at the higher position (S 4-5) than that at the lower position (S 1-2). This was due to the fact that as the axial height ascended, the size of the rising bubble became larger and the associated rising velocity became faster. Since the motion of rising bubbles was the source of particle motions within the bed, the average particle velocity also increased and the particle motion became more energetic. The average correlation velocity of particle clouds could be used as a parameter to measure the magnitude of particle velocity in the dense-phase region of the fluidized bed. Table 2 further displayed the average correlation velocity measured under different superficial gas velocities at four axial positions. The measurement process was repeated three times under each superficial gas velocity. The correlation velocities shown in Table 2 were the mean values of the three average correlation velocities mentioned previously. The relative error was no more than 12.7%, which is greater than that in the dilute pneumatic conveying system [19]. The reason is that distributions of particle velocity and concentration in fluidized beds are much more distinct than those in the dilute pneumatic conveying system and which make the increases of relative errors of measured results. The experimental results shown in Fig. 8 and Table 2 demonstrated that electrostatic sensors combined with cross-correlation method are capable of providing reliable velocity measurement with good repeatability in the dense-phase region of the fluidized bed. Besides, the four pairs of electrostatic sensors installed at a certain height provided nearly the same average correlation velocity and normalized probability density distributions of correlation velocities, which was similar with our previous experimental work [46]. This uniformity means that at a certain axial height, the measured average correlation velocity of particle clouds from only one pair of electrostatic sensors could be used to represent the intensity of particle motions in this section.

Fig. 9 further compares the average correlation velocity of particle clouds with the theoretical

bubble rise velocity estimated by Eq. (4), where the dash lines represent the bubble velocity and the solid points stand for the average correlation velocity. As shown in Fig. 9, the same tendency was observed for the bubble rise velocity and the average correlation velocity of particle clouds as the superficial gas velocity increased. Both the theoretical bubble velocity and the experimental average correlation velocity ascended with the superficial gas velocity. This verifies again that the average correlation velocity of particle clouds can be used to reflect the relative magnitude of particle motions affected by rising bubbles. It should be noticed that all the measured average correlation velocities were positive in the dense-phase region in the fluidized bed, which means that particle clouds mainly moved upward during the measurement. Moreover, the average correlation velocity measured at the higher position (S 6-7) of the dense-phase region was always smaller than that measured at a lower position (S 4-5), which was different from the comparison result from S 1-2 and S 4-5.

It can be found from the previous research [20] that the sensitivity zone of the arc-shape electrode was localized and the measurement by the electrodes was more sensitive to the charged particles near the electrode. It is also known that particles near the wall mainly move downward in the gas-solid fluidized bed [47-49]. Therefore, it is prone to infer that the correlation velocity measured by the arc-shape electrostatic sensors on the outer wall of the fluidized bed should be negative, which represents that particles mainly move downward. However, the experimental result obtained in this work is not the case as inferred, which is mainly attributed to the following facts during fluidization. The net downward transport of particles is only in the wall region in the fluidized bed, whereas the overall upward flow of particle motions occupies the remaining larger part of the cross section [24]. Furthermore, the magnitude of upward velocity is remarkably greater than that of the downward velocity [47, 50]. Since the induced electrostatic voltage was simultaneously affected by spatial sensitivity of sensors and particle velocity, the measured correlation velocity was always positive in the dense-phase region in the fluidized bed, which means particles showed an overall upward movement in this region. While for the dynamic bed level region, both the upward and downward particle motions were more vigorous [50]. The number of particles moving upward became fewer since more particles moved laterally due to the bubbles eruption at the bed surface [24]. As a result, the upward and downward particle movements could be detected simultaneously in this region as shown below.

In the dynamic bed level region, particles are thrown into the freeboard region by erupted rising bubbles and finally fall into the bed again under gravity. Combined with the specific dynamic bed level ranges shown in Table 3, Fig. 10 further illustrates the relative positions of the dynamic bed level and fixed electrostatic sensors under different gas velocities, where the blue dash lines represent the average top and bottom edges of the dynamic bed level. Fig. 11 shows the probability density distributions of the correlation velocities measured by S 8-9 in the bed level region with gas velocity increasing. It can be indicated that when the gas velocity was relatively small ($u=0.4$ m/s), the sensors pair S 8-9 was near the top edge of the dynamic level region. The average correlation velocity was negative and the distribution of the correlation velocities was also mainly located in the negative direction, which means that particles primarily moved downward in the upper part of the bed level region. Since the position of the sensors pair was fixed but the dynamic bed level ascended due to the increase of gas velocity, the section measured by S 8-9 gradually approached the bottom edge of the dynamic level region, until it belonged to the intersection between the bed level and dense-phase regions, where particles were mainly thrown upward by erupted bubbles. As a result, both the number of particles moving upward and the value of upward velocity increased in comparison with the situation under a lower superficial gas velocity. Therefore, distributions of the correlation velocities measured by S 8-9 were located in both the negative and positive directions, and positive correlation velocities became more prominent with the increase of superficial gas velocity. When the gas velocity became larger ($u=0.7$ m/s), the distribution of correlation velocities was quite similar with that in the dense-phase region of the fluidized bed. Fig. 12 displayed the variations of probability density distributions of correlation velocities measured by different pairs of sensors under a certain gas velocity. When the superficial gas velocity was 0.5 m/s (Fig. 10(b)), S 8-9 belonged to the middle of the dynamic level region, where both positive and negative correlation velocities could be detected. While for S 9-10 located near the top edge of the dynamic level range, the distribution of correlation velocities dominantly lay in the negative direction. When the superficial gas velocity increased to 0.7 m/s (Fig. 10(d)), sensors S 8-10 were in the intersection of the bed level and dense-phase regions while S 11-12 was located in the upper part of the dynamic bed level region. Distributions of correlation velocities measured by S 8-9 and S 9-10 were similar to those in the dense-phase region of the fluidized bed, while negative correlation velocities appeared as the position of the sensors pair

became higher (S 11-12).

In a word, both upward and downward movements of particles could be measured in the dynamic bed level regions, which is different from the results obtained in the dense-phase region of the fluidized bed. In the dynamic bed level region, the numbers and velocities of particles moving upward and downward were always changing due to the complex velocity and concentration distributions of particles, and both positive and negative correlation velocities could be detected. This also gives a probable explanation to the unusual result shown in Fig. 9. Since the position of S 6-7 was closer to the dynamic bed level, the downward movement of particles near the wall was more vigorous than that in the lower part of the dense-phase region [24]. Consequently, the average correlation velocity in the higher position (S 6-7) was smaller than that in the lower position (S 4-5).

Based on the experimental results from the dense-phase and dynamic bed level regions of the fluidized bed, it can be inferred that the average correlation velocity of particle clouds obtained by electrostatic sensors combined with cross-correlation method can be used as a parameter to reflect the relative magnitude of particle velocity and intensity of particle motions. Furthermore, a positive correlation velocity means upward motions of particles are dominant and a negative correlation velocity represents an overall downward movement of particles. The measurement results verified the repeatability and reliability of electrostatic sensors to monitor particle motions in the gas-solid fluidized bed.

4.2. Comparison of fluidization characteristics of Geldart B and D particles

The criteria to select the parameters in the cross-correlation calculation for Geldart D particles are the same with those for Geldart B particles, which are hence not described in detail in this section. The integral time (T) was also chosen as 2 s and only the correlation velocity associated with a maximum correlation coefficient greater than 0.6 was regarded as a valid result. For Geldart D particles, the ratio of maximum coefficients over 0.6 was no less than 95% in this experiment, which demonstrated the remarkable correlation between the upstream and downstream electrostatic signals in the fluidized bed with Geldart D particles. The probability density distributions of correlation velocities of Geldart D particle clouds are shown in Fig. 13. The correlation velocity distribution broadened and the magnitude of the correlation velocity

corresponding to the peak became greater with the increase of superficial gas velocity. Since bubbles grow up and coalesce as they rise along the axial height within the fluidized bed, particles motions carried by larger bubbles become more energetic. Therefore, the distribution of correlation velocities with the axial height became broader with a larger average correlation velocity as shown in Fig. 13(b).

Fig. 14 further compares the average correlation velocity and the theoretical bubble rise velocity at different heights under various superficial gas velocities. The average correlation velocity and theoretical bubble rise velocity showed a similar tendency with the increase of gas velocity at different axial heights. The experimental results shown in Figs. 13 and 14 demonstrated the applicability of the cross-correlation method based on electrostatic signals in the fluidized bed with Geldart D particles.

When the dimensions of the fluidized bed are fixed, the bubble size and rise velocity depend on the excess gas velocity ($u-u_{mf}$) and the ratio of gas in the bubble phase [51], which significantly affect particle motions. In order to compare and analyze the fluidization characteristics of Geldart B and D particles, Fig. 15 displays the average correlation velocity of Geldart D and B particles at two axial heights under the same excess gas velocity. It can be found that the average correlation velocity of Geldart B particles was significantly greater than that of Geldart D particles under the same excess gas velocity. To be specific, when the excess velocity was 0.35 m/s, the average correlation velocities measured by S 4-5 were 0.451 m/s and 0.586 m/s for Geldart D and B particles, respectively. The average correlation velocity of Geldart B particles was 29.9 percent greater than that of Geldart D particles under this condition. Within the experimental conditions covered by this work, the average correlation velocity of Geldart B particles was 20-40 percent larger than that of Geldart D particles. Fig. 16 further compares the normalized correlation velocity distributions of Geldart B and D particles. Under the same excess gas velocity, the normalized correlation velocity distribution of Geldart B was broader than that of Geldart D particles at a certain height and the correlation velocity corresponding to the peak was also greater. These experimental results demonstrated that motions of Geldart B particles were obviously more vigorous than Geldart D particles under the same excess gas velocity.

The difference of particle motions shown in Figs. 15 and 16 is due to the distinction of fluidization characteristics of different Geldart types particles. In a fluidized bed with Geldart B

particles, bubbles coalescence is more predominant than bubbles split [52]. As a result, the size of bubbles keeps enlarging as they rise along the axial height of the bed and the rise velocity of bubbles increases. For the fluidized bed with Geldart D particles, the rise velocity of bubbles within the bed is always smaller than the gas velocity in the emulsion phase (u_{mf}/ε_{mf}) due to the large minimum fluidization velocity of Geldart D particles. Consequently, the gas in the emulsion phase can flow into the bubble from the bottom and flow out from the top, which makes the bubble split and become smaller [52]. The average size and rise velocity of bubbles in the fluidized bed with Geldart D particles are always smaller than those in the fluidized bed with Geldart B particles. Movements of Geldart B particles carried by larger rising bubbles are therefore more intensive than Geldart D particles. Moreover, although it is believed that all the gas exceeding the minimum fluidization velocity, namely, $u-u_{mf}$, will contribute to the bubble formation according to the classical two-phase theory, actually, some of the gas expected to go through the bed as bubbles does not [51]. Previous research [53] has indicated that the ratios of gas forming bubbles to the gas expected to form bubbles are 0.65 and 0.26 for Geldart B and D particles, respectively. This means that the volume of gas which goes through the bed as bubbles is significantly smaller for Geldart D particles than for Geldart B particles. The ratio of gas forming bubbles actually also leads to the less vigorous movements of Geldart D particles. Therefore, the developed monitoring method can be used to characterize and distinguish the motions and fluidization behaviors of particles of different types.

5. Conclusions

Induced electrostatic voltage signals were measured by arc-shape electrostatic sensors installed on the outer wall of the fluidized bed in this work. The average correlation velocity of particles and the normalized probability density distributions of correlation velocities were obtained and compared under various fluidization conditions for Geldart B and D particles. The reliability and repeatability of velocity measurement by electrostatic sensors combined with cross-correlation method in the gas-solid fluidized bed were demonstrated and the fluidization characteristic differences of Geldart B and D particles were further compared and illustrated.

For Geldart B particles in the dense-phase region of the fluidized bed, with the increase of superficial gas velocity or the axial height, the average correlation velocity of particle clouds

increased and the normalized probability density distributions of correlation velocities broadened. The variation of the average correlation velocity showed the similar trend with the theoretical bubble rise velocity. The average correlation velocity was always positive due to the relatively greater velocity and larger proportion of particles moving upward carried by rising bubbles in the dense-phase region. The average correlation velocities measured showed a good repeatability with a relative error no more than 12.7%. In the dynamic bed level region, both upward and downward correlation velocities could be detected for the complex particle velocity and concentration distributions in this region. The experimental results verified that the average correlation velocity and the distribution of correlation velocities can be used to reflect the direction and intensity of particle motions at a certain height in the gas-solid fluidized bed.

For Geldart D particles, the velocity measurement based on electrostatic sensors and cross-correlation method was still applicable. Moreover, compared with Geldart B particles, the average correlation velocity of Geldart D particles was smaller and the normalized probability density distribution of correlation velocities was narrower under the same excess velocity. This was caused by the differences of fluidization behaviors between these two types of particles. More gas goes through the bed as bubbles and coalescence of bubbles is more predominant in the fluidized bed with Geldart B particles than that with Geldart D particles. Therefore, particle movements mainly driven by larger bubbles were more vigorous in the fluidized bed with Geldart B particles.

Considering the simplicity, cost effectiveness and non-invasiveness, this method is a potential and promising method to characterize particle motions in the fluidized bed. However, due to the fact that particle motions, particle charging and concentration distribution are quite complex in the fluidized bed, a more explicit physical interpretation of correlation velocity in the fluidized bed, effects of particle velocity and concentration distributions on correlation velocity measurement, and the optimization of sensor configurations, still need more investigation in the future work.

Notations

d_b	bubble diameter, m
d_{b0}	initial bubble diameter formed at the surface of the perforated distributor, m
d_t	inner diameter of the fluidized bed, m

f	sampling frequency, Hz
H	axial distance of electrostatic sensor from the distributor, mm
K	meter factor, dimensionless
L	distance between the centers of adjacent electrostatic sensors, mm
N_0	the number of holes in the distributor
R	cross-correlation coefficient, dimensionless
t	time, s
T	integral time in the cross-correlation calculation, s
u	superficial gas velocity, m/s
u_{mf}	minimum fluidization velocity, m/s
v_c	particle correlation velocity, m/s
v_m	particle mean velocity, m/s
x	upstream electrostatic voltage signal, V
y	downstream electrostatic voltage signal, V
z	axial distance of bubbles from the distributor, m
<i>Greek letters</i>	
τ	time lag, s
τ_0	the first zero crossing point in the auto-correlation function of electrostatic signals, s
τ_m	transit time, s

Acknowledgement

The authors are grateful for the financial support of this work by the National Natural Science Foundation of China (No. 21236007), the National Science Fund for Distinguished Young (21525627), the National Natural Science Foundation of China (No. 61403138), the Natural Science Foundation of Zhejiang Province (Grant No. LR14B060001) and the Specialized Research Fund for the Doctoral Program of Higher Education (Grant 20130101110063).

References

- [1] X. Fan, D.J. Parker, Z. Yang, J.P.K. Seville, J. Baeyens, The effect of bed materials on the solid/bubble motion in a fluidised bed, *Chemical Engineering Science*, 63 (2008) 943-950.
- [2] G. Hendrickson, Electrostatics and gas phase fluidized bed polymerization reactor wall sheeting, *Chemical Engineering Science*, 61 (2006) 1041-1064.
- [3] J. Ciborowski, A. Wlodarski, On electrostatic effects in fluidized beds, *Chemical Engineering Science*, 17 (1962) 23-32.
- [4] R.G. Rokkam, R.O. Fox, M.E. Muhle, Computational fluid dynamics and electrostatic modeling of polymerization fluidized-bed reactors, *Powder Technology*, 203 (2010) 109-124.

- [5] M. Glor, Hazards due to electrostatic charging of powders, *Journal of Electrostatics*, 16 (1985) 175-191.
- [6] Y. Zhang, Y.C. Liang, C.H. Wang, Hazard of electrostatic generation in a pneumatic conveying system: electrostatic effects on the accuracy of electrical capacitance tomography measurements and generation of spark, *Meas. Sci. Technol.*, 19 (2008) 1-10.
- [7] J. Li, F.Z. Xiao, Z.H. Luo, A CFD modeling of the gas-solid two-phase flow in an FCC riser under the electrostatic conditions, *Asia-Pacific Journal of Chemical Engineering*, 9 (2014) 645-655.
- [8] H.T. Bi, A. Chen, J.R. Grace, Monitoring electrostatic charges in fluidized beds, *ECI Conference on "The 12th International Conference on Fluidization-New Horizons in Fluidization Engineering"* Vancouver, 2007, pp. 1001-1008.
- [9] C. He, X.T. Bi, J.R. Grace, Decoupling electrostatic signals from gas-solid bubbling fluidized beds, *Powder Technology*, 290 (2016) 11-20.
- [10] F. Jalalinejad, X.T.T. Bi, J.R. Grace, Effect of electrostatic charges on single bubble in gas-solid fluidized beds, *International Journal of Multiphase Flow*, 44 (2012) 15-28.
- [11] A. Giffin, P. Mehrani, Effect of gas relative humidity on reactor wall fouling generated due to bed electrification in gas-solid fluidized beds, *Powder Technology*, 235 (2013) 368-375.
- [12] M.A. Hassani, R. Zarghami, H.R. Norouzi, N. Mostoufi, Numerical investigation of effect of electrostatic forces on the hydrodynamics of gas-solid fluidized beds, *Powder Technology*, 246 (2013) 16-25.
- [13] K. Dong, Q. Zhang, Z. Huang, Z. Liao, J. Wang, Y. Yang, Experimental investigation of electrostatic effect on bubble behaviors in gas-solid fluidized bed, *AIChE Journal*, 61 (2015) 1160-1171.
- [14] K. Dong, Q. Zhang, Z. Huang, Z. Liao, J. Wang, Y. Yang, F. Wang, Experimental investigation of electrostatic effect on particle motions in gas-solid fluidized beds, *AIChE Journal*, 61 (2015) 3628-3638.
- [15] Z. Qing, D. Kezeng, Z. Yefeng, H. Zhengliang, L. Zuwei, W. Jingdai, Y. Yongrong, W. Fang, A comparative study of electrostatic current and pressure signals in a MSFC gas-solid fluidized bed, *Powder Technology*, 287 (2016) 292-300.
- [16] C. He, X.T. Bi, J.R. Grace, Contact electrification of a novel dual-material probe with charged particulate flow, *Powder Technology*, 253 (2014) 1-9.
- [17] C. He, X.T. Bi, J.R. Grace, Simultaneous measurements of particle charge density and bubble properties in gas-solid fluidized beds by dual-tip electrostatic probes, *Chemical Engineering Science*, 123 (2015) 11-21.
- [18] C. He, X.T. Bi, J.R. Grace, Monitoring Electrostatics and Hydrodynamics in Gas-Solid Bubbling Fluidized Beds Using Novel Electrostatic Probes, *Industrial & Engineering Chemistry Research*, 54 (2015) 8333-8343.
- [19] Y. Yan, B. Byrne, S. Woodhead, J. Coulthard, Velocity measurement of pneumatically conveyed solids using electrodynamic sensors, *Meas. Sci. Technol.*, 6 (1995) 515-537.
- [20] W.B. Zhang, Y.P. Cheng, C. Wang, W.Q. Yang, C.H. Wang, Investigation on hydrodynamics of triple-bed combined circulating fluidized bed using electrostatic sensor and electrical capacitance tomography, *Industrial & Engineering Chemistry Research*, 52 (2013) 11198-11207.
- [21] C. Xu, B. Zhou, D. Yang, G. Tang, S. Wang, Velocity measurement of pneumatically conveyed solid particles using an electrostatic sensor, *Meas. Sci. Technol.*, 19 (2008) 1-9.
- [22] C.L. Xu, B. Zhou, S.M. Wang, Dense-phase pneumatically conveyed coal particle velocity

- measurement using electrostatic probes, *Journal of Electrostatics*, 68 (2010) 64-72.
- [23] C. Liang, C.S. Zhao, X.P. Chen, W.H. Pu, P. Lu, C.L. Fan, Flow characteristics and Shannon entropy analysis of dense-phase pneumatic conveying of pulverized coal with variable moisture content at high pressure, *Chemical Engineering & Technology*, 30 (2007) 926-931.
- [24] M. Stein, Y.L. Ding, J.P.K. Seville, D.J. Parker, Solids motion in bubbling gas fluidised beds, *Chemical Engineering Science*, 55 (2000) 5291-5300.
- [25] D.J. Parker, C.J. Broadbent, P. Fowles, M.R. Hawkesworth, P. McNeil, Positron emission particle tracking - a technique for studying flow within engineering equipment, *Nuclear Instruments and Methods in Physics Research Section A: Accelerators, Spectrometers, Detectors and Associated Equipment*, 326 (1993) 592-607.
- [26] L. Li, A. Rasmuson, A. Ingram, M. Johansson, J. Rempelgas, C. von Corswant, S. Folestad, PEPT Study of Particle Cycle and Residence Time Distributions in a Wurster Fluid Bed, *AIChE Journal*, 61 (2015) 756-768.
- [27] D.J. Parker, A.E. Dijkstra, T.W. Martin, J.P.K. Seville, Positron emission particle tracking studies of spherical particle motion in rotating drums, *Chemical Engineering Science*, 52 (1997) 2011-2022.
- [28] N. Mostoufi, J. Chaouki, Local solid mixing in gas–solid fluidized beds, *Powder Technology*, 114 (2001) 23-31.
- [29] C.R. Müller, J.F. Davidson, J.S. Dennis, A.N. Hayhurst, A Study of the Motion and Eruption of a Bubble at the Surface of a Two-Dimensional Fluidized Bed Using Particle Image Velocimetry (PIV), *Industrial & Engineering Chemistry Research*, 46 (2007) 1642-1652.
- [30] Jan Albert Laverman, Ivo Roghair, Martin van Sint Annaland, H. Kuipers., Investigation into the hydrodynamics of gas-solid fluidized beds using particle image velocimetry coupled with digital image analysis, *The Canadian Journal of Chemical Engineering*, 86 (2008) 523-535.
- [31] F. Hamdullahpur, G.D.M. MacKay, Two-phase flow behavior in the freeboard of a gas-fluidized bed, *AIChE Journal*, 32 (1986) 2047-2055.
- [32] A. Mychkovsky, D. Rangarajan, S. Ceccio, LDV measurements and analysis of gas and particulate phase velocity profiles in a vertical jet plume in a 2D bubbling fluidized bed: Part I: A two-phase LDV measurement technique, *Powder Technology*, 220 (2012) 55-62.
- [33] J.J. Nieuwland, R. Meijer, J.A.M. Kuipers, W.P.M. vanSwaij, Measurements of solids concentration and axial solids velocity in gas-solid two-phase flows, *Powder Technology*, 87 (1996) 127-139.
- [34] Haiyan Zhu, Jesse Zhu, Guozheng Li, F. Li., Detailed measurements of flow structure inside a dense gas–solids fluidized bed, *Powder Technology*, 180 (2008) 339-349.
- [35] J. Wang, C. Ren, Y. Yang, L. Hou, Characterization of Particle Fluidization Pattern in a Gas Solid Fluidized Bed Based on Acoustic Emission (AE) Measurement, *Industrial & Engineering Chemistry Research*, 48 (2009) 8508-8514.
- [36] J. Wang, C. Ren, Y. Yang, Characterization of Flow Regime Transition and Particle Motion Using Acoustic Emission Measurement in a Gas-Solid Fluidized Bed, *AIChE Journal*, 56 (2010) 1173-1183.
- [37] T. Hagemeyer, M. Börner, A. Bück, E. Tsotsas., A comparative study on optical techniques for the estimation of granular flow velocities, *Chemical Engineering Science*, 131 (2015) 63-75.
- [38] Sina Tebianian, Kristian Dubrawski, Naoko Ellis, Ray A. Cocco, Roy Hays, S.B. Reddy Karri, Thomas W. Leadbeater, David J. Parker, Jamal Chaouki, Rouzbeh Jafari, Pablo Garcia-Trinanes, Jonathan P.K. Seville, J.R. Grace, Investigation of particle velocity in FCC gasfluidized beds based on different measurement techniques, *Chemical Engineering Science*, 127 (2015) 310-322.

- [39] J. Werther, Measurement techniques in fluidized beds, *Powder Technology*, 102 (1999) 15-36.
- [40] W.B. Zhang, C. Wang, Y.L. Wang, Parameter selection in cross-correlation based velocimetry using circular electrostatic sensors, *Ieee Transactions on Instrumentation and Measurement*, 59 (2010) 1268-1275.
- [41] C.L. Xu, C. Liang, B. Zhou, S.M. Wang, HHT analysis of electrostatic fluctuation signals in dense-phase pneumatic conveying of pulverized coal at high pressure, *Chemical Engineering Science*, 65 (2010) 1334-1344.
- [42] X. Fan, Z. Yang, D.J. Parker, B. Armstrong, Prediction of bubble behaviour in fluidised beds based on solid motion and flow structure, *Chemical Engineering Journal*, 140 (2008) 358-369.
- [43] Davidson J F, H. D., *Fluidized particles*, Cambridge University Press, New York, 1963.
- [44] S. Mori, C.Y. Wen, Estimation of bubble diameter in gaseous fluidized beds, *AIChE Journal*, 21 (1975) 109-115.
- [45] X. Ling'an, *Cross-Correlation Flow Measurement Technique*, Tianjin University Press, Tianjn, 1988.
- [46] W.B. Zhang, Y. Yan, Y.R. Yang, J.D. Wang, Measurement of flow parameters in a bubbling fluidized bed using electrostatic sensor arrays, *IEEE International Instrumentation and Measurement Technology Conference (I2MTC 2015)Pisa, Italy*, 2015.
- [47] S. Harms, S. Stapf, B. Blumich, Application of k- and q-space encoding NMR techniques on granular media in a 3D model fluidized bed reactor, *Journal of Magnetic Resonance*, 178 (2006) 308-317.
- [48] H.L. Lu, Y.H. Zhao, J.M. Ding, D. Gidaspow, L. Wei, Investigation of mixing/segregation of mixture particles in gas-solid fluidized beds, *Chemical Engineering Science*, 62 (2007) 301-317.
- [49] J. Min, J.B. Drake, T.J. Heindel, R.O. Fox, Experimental Validation of CFD Simulations of a Lab-Scale Fluidized-Bed Reactor with and Without Side-Gas Injection, *AIChE Journal*, 56 (2010) 1434-1446.
- [50] G.A. Bokkers, J.A. Laverman, M.V. Annaland, J.A.M. Kuipers, Modelling of large-scale dense gas-solid bubbling fluidised beds using a novel discrete bubble model, *Chemical Engineering Science*, 61 (2006) 5590-5602.
- [51] K. Daizo, O. Levenspiel, *Fluidization Engineering*, Butterworth, Boston, 1991.
- [52] Gantang Chen, Z. Wang, *Multiphase Flow Reaction Engineering*, Zhejiang University Press, Hangzhou, 1996.
- [53] K. Hillegardt, J. Werther, Local bubble gas hold-up and expansion of gas/solid fluidized beds, *German Chemical Engineering*, 9 (1986) 215-221.

No.	Figure captions
Figure 1	Schematic diagram of the experimental apparatus.
Figure 2	Installation layout of arc-shaped electrostatic sensors.
Figure 3	Induced electrostatic voltage signals from adjacent sensors and corresponding PSDs. (S 4-5, $u=0.5$ m/s)
Figure 4	Cross-correlation coefficients of induced electrostatic signals from adjacent sensors in the fluidized bed of Geldart B particles. (S 4-5, $u=0.5$ m/s)
Figure 5	Variations of STDs of correlation velocity with integral time.
Figure 6	Cross-correlation results of upstream and downstream electrostatic signals. (S 4-5) (a) Correlation coefficient; (b) Correlation velocity
Figure 7	Normalized probability density distributions of particle cloud correlation velocities under different superficial gas velocities. (S 4-5)
Figure 8	Variation of average particle cloud correlation velocity with superficial gas velocity.
Figure 9	Comparison of average correlation velocity of Geldart B particle clouds and theoretical bubble rise velocity.
Figure 10	Schematic of relative positions of electrostatic sensors and dynamic bed level. (a) $u=0.4$ m/s; (b) $u=0.5$ m/s; (c) $u=0.6$ m/s; (d) $u=0.7$ m/s
Figure 11	Normalized probability density distributions of particle cloud correlation velocities in the bed-level region of the fluidized bed. (S 8-9)
Figure 12	Variations of particle cloud correlation velocity distributions with axial height in the bed-level region of the fluidized bed. (a) $u=0.5$ m/s; (b) $u=0.7$ m/s
Figure 13	Variations of correlation velocity distributions of Geldart D particle clouds with superficial gas velocity and axial height. (a) S 4-5; (b) $u=0.9$ m/s
Figure 14	Comparison of average correlation velocity of Geldart D particle clouds with theoretical bubble rise velocity.
Figure 15	Average correlation velocities of Geldart B and D particles under different excess superficial gas velocities.
Figure 16	Comparison of correlation velocity distributions of Geldart B and D particles. (a) $u-u_{mf}=0.15$ m/s; (b) $u-u_{mf}=0.35$ m/s

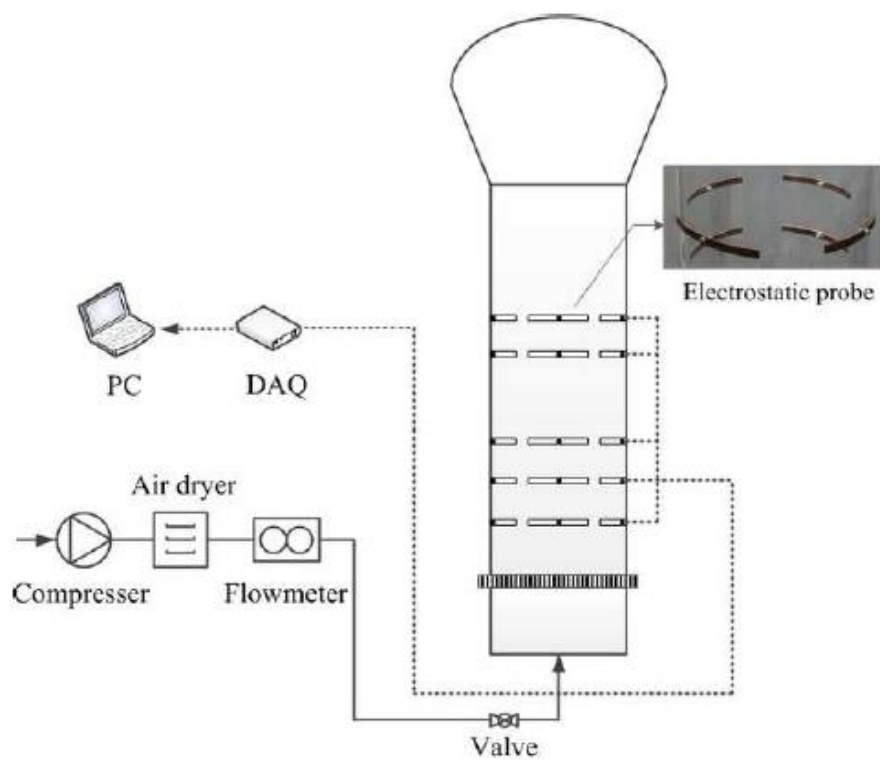


Fig. 1

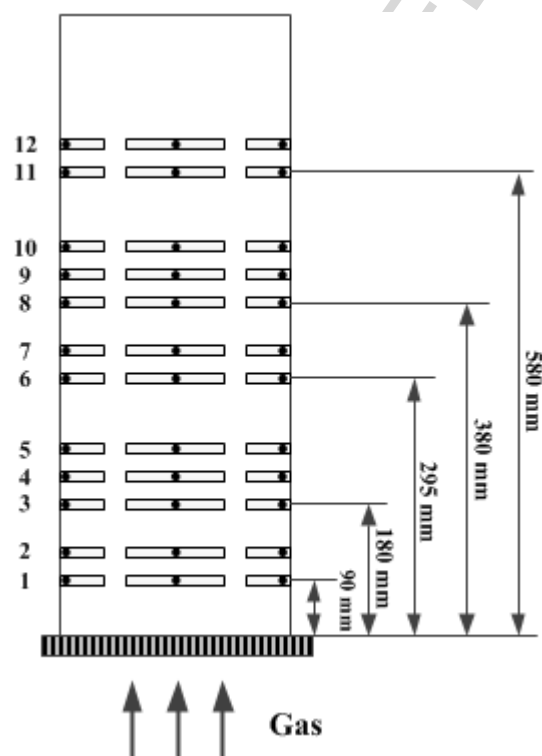


Fig. 2

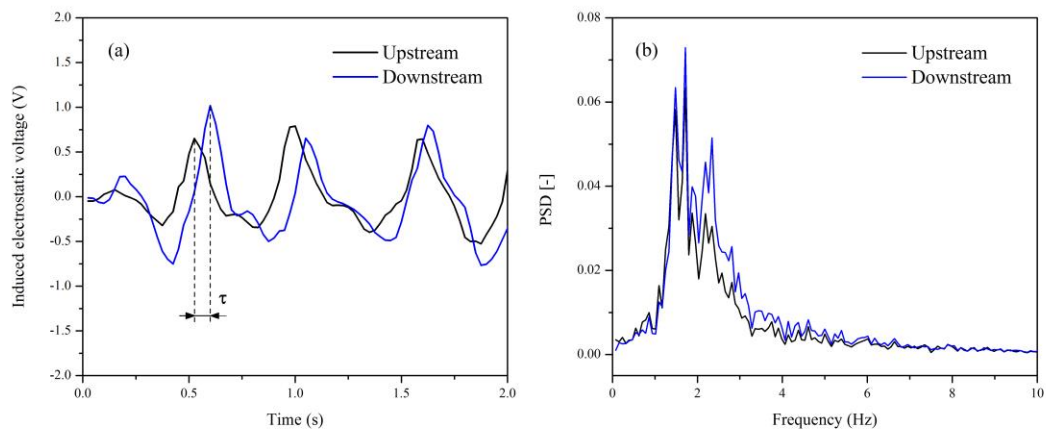


Fig. 3

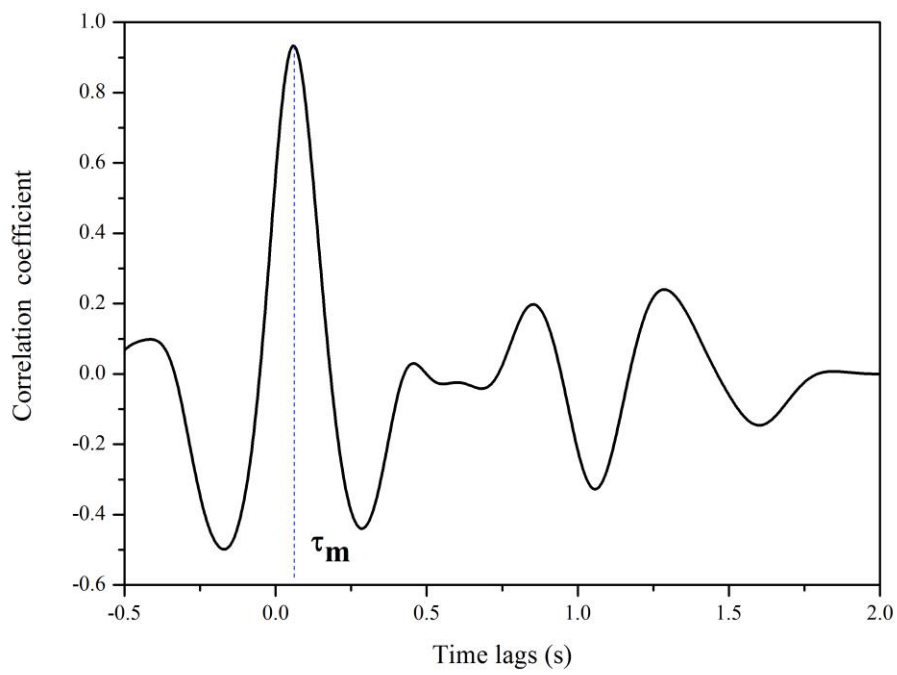


Fig. 4

ACCEPTED

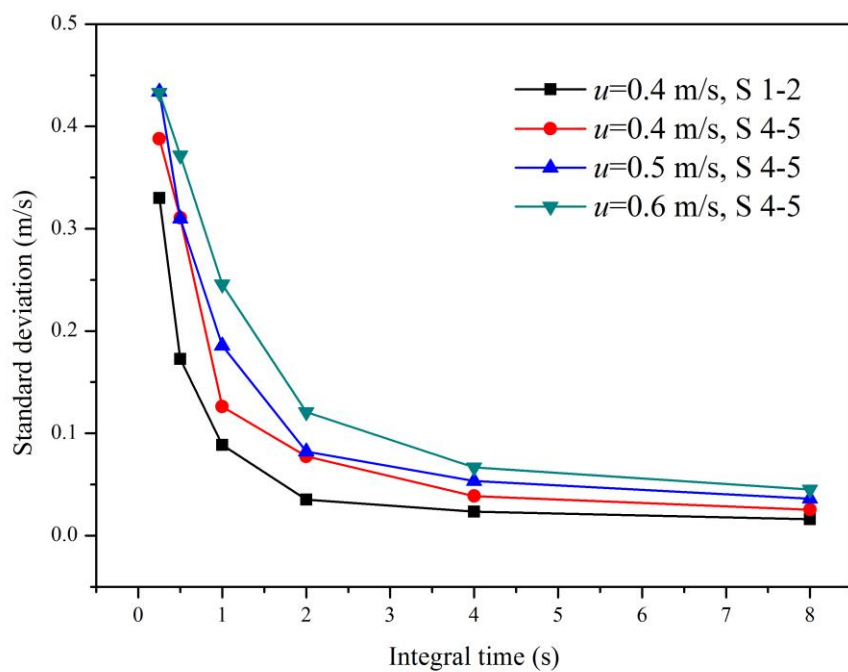


Fig. 5

ACCEPTED

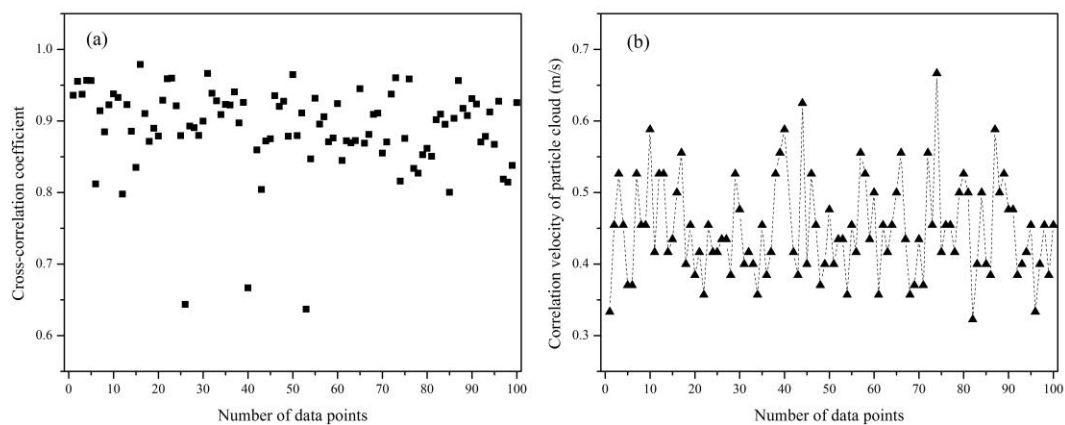


Fig. 6

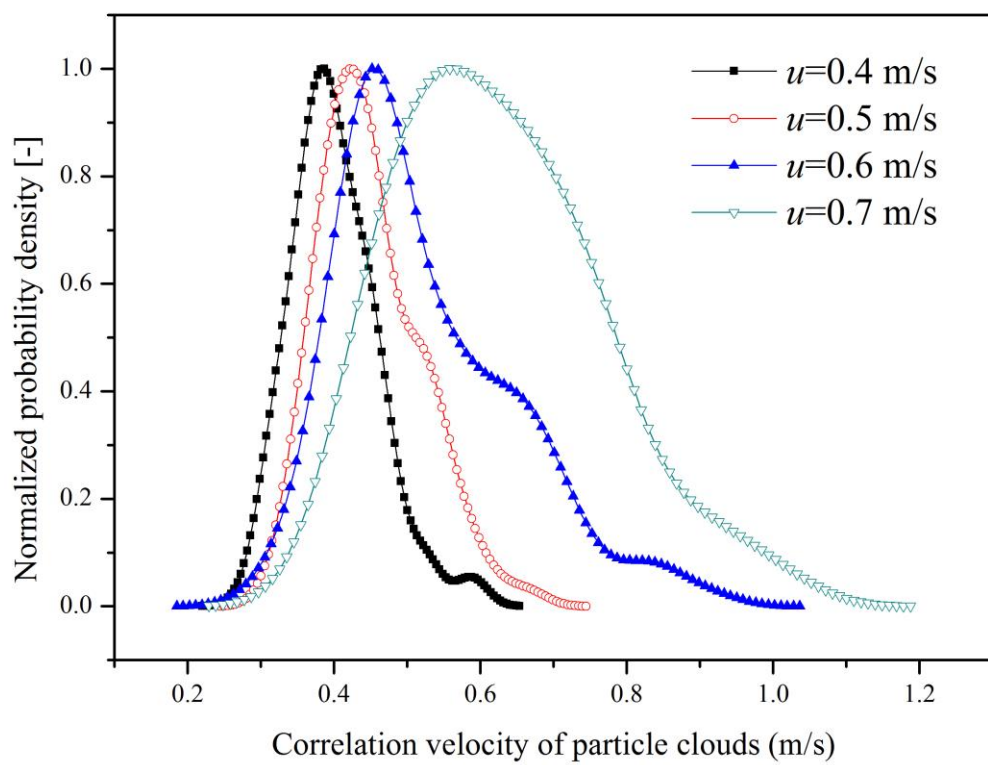


Fig. 7

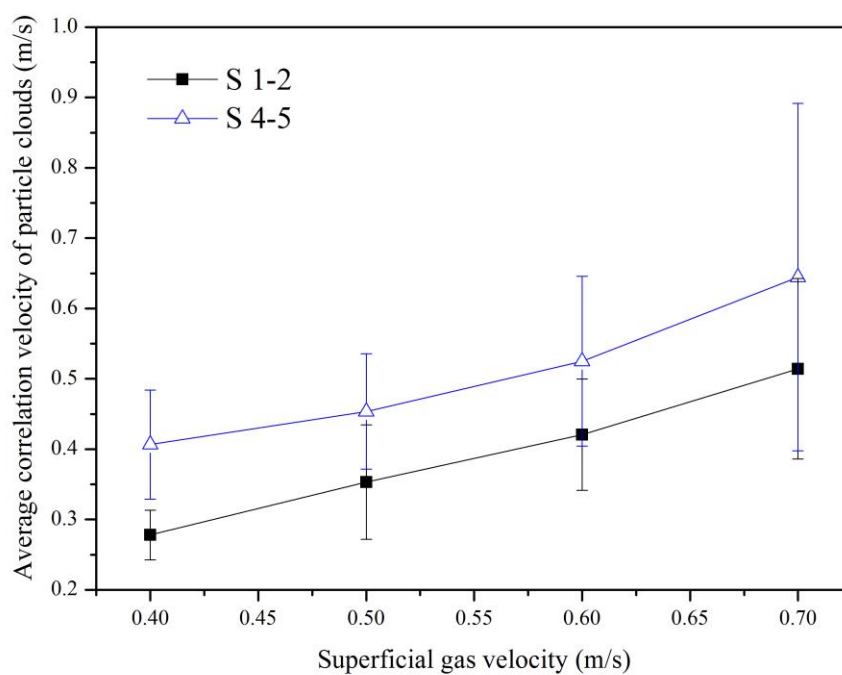


Fig. 8

ACCEPTED

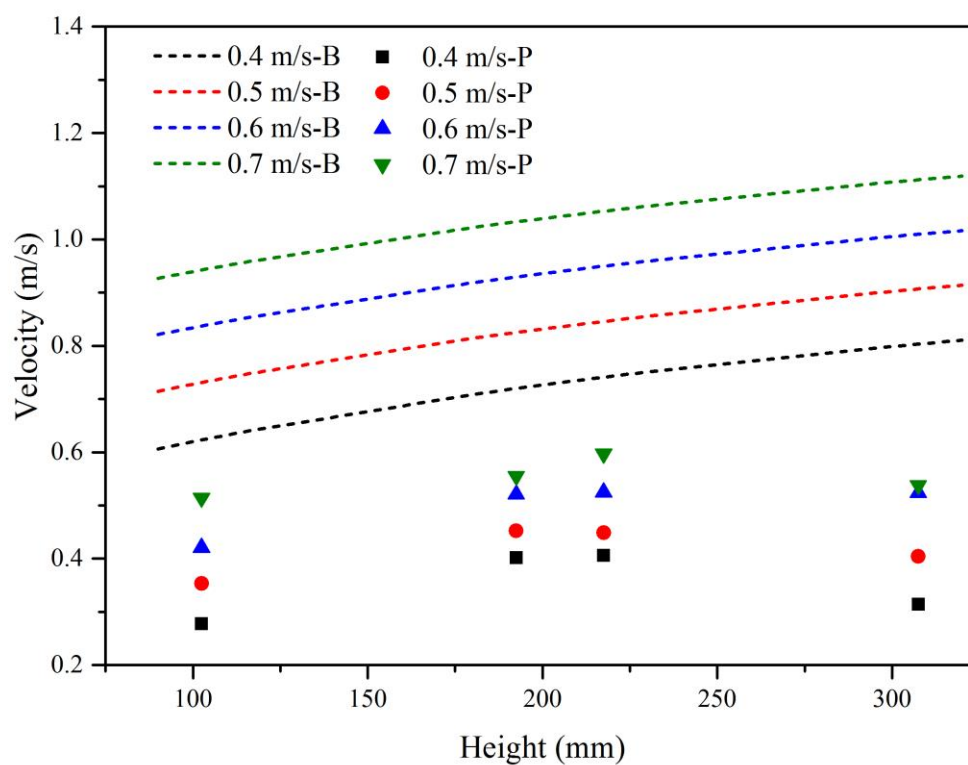


Fig. 9

ACCEPTED

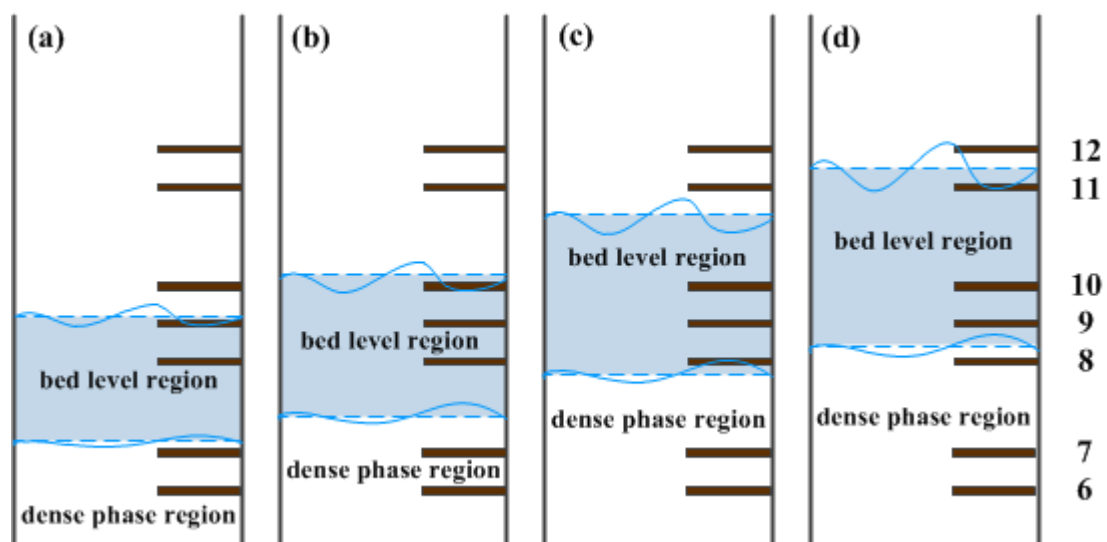


Fig. 10

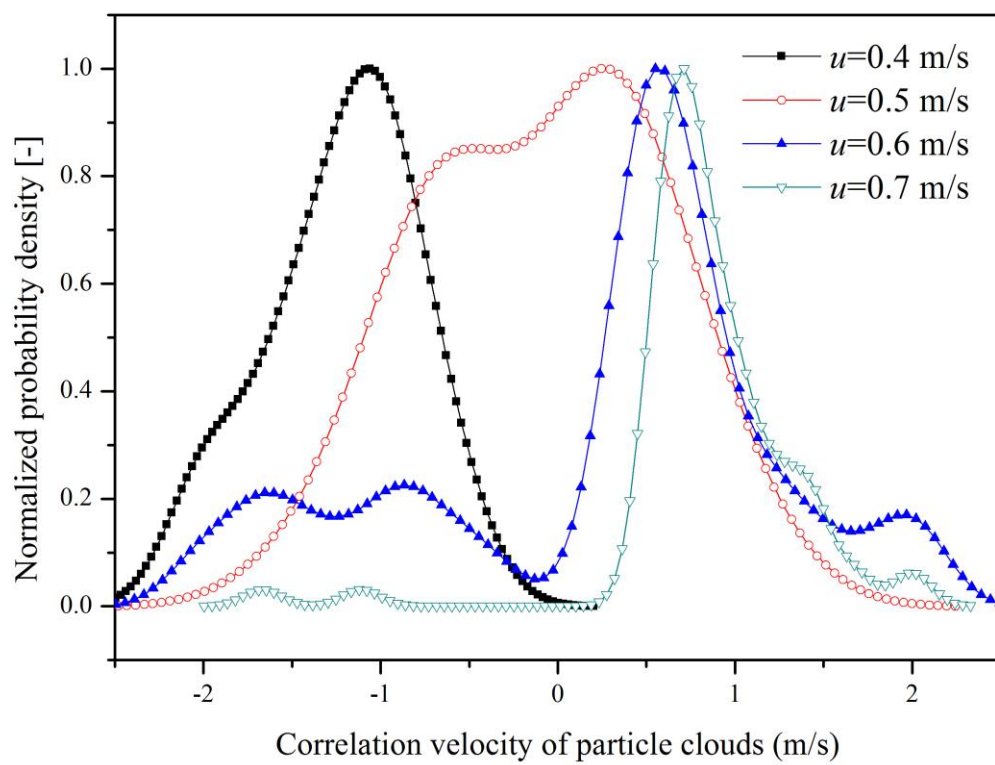


Fig. 11

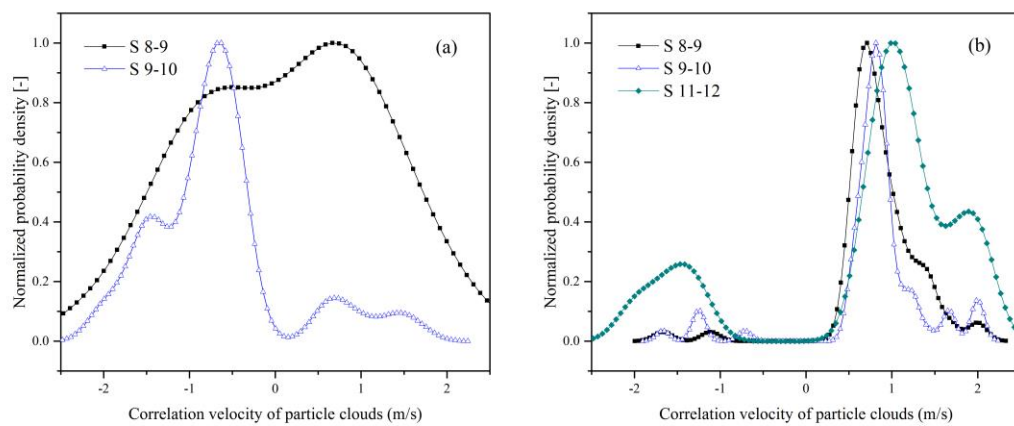


Fig. 12

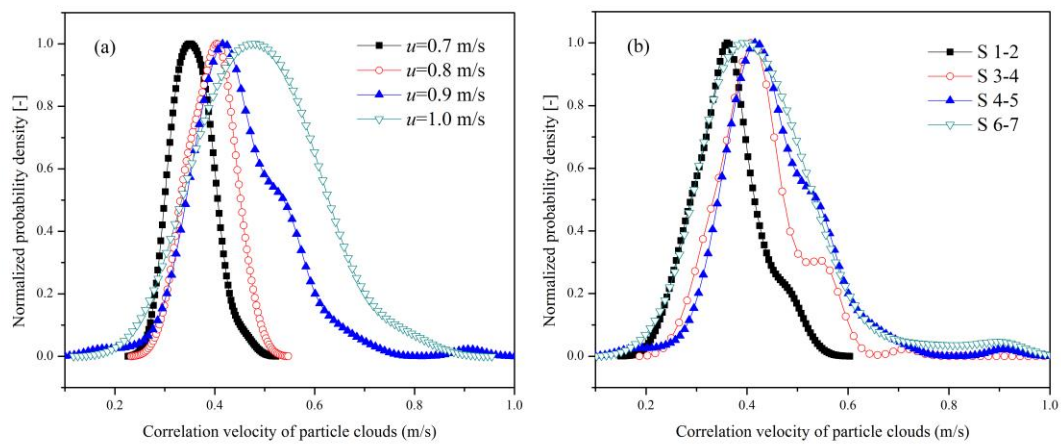


Fig. 13

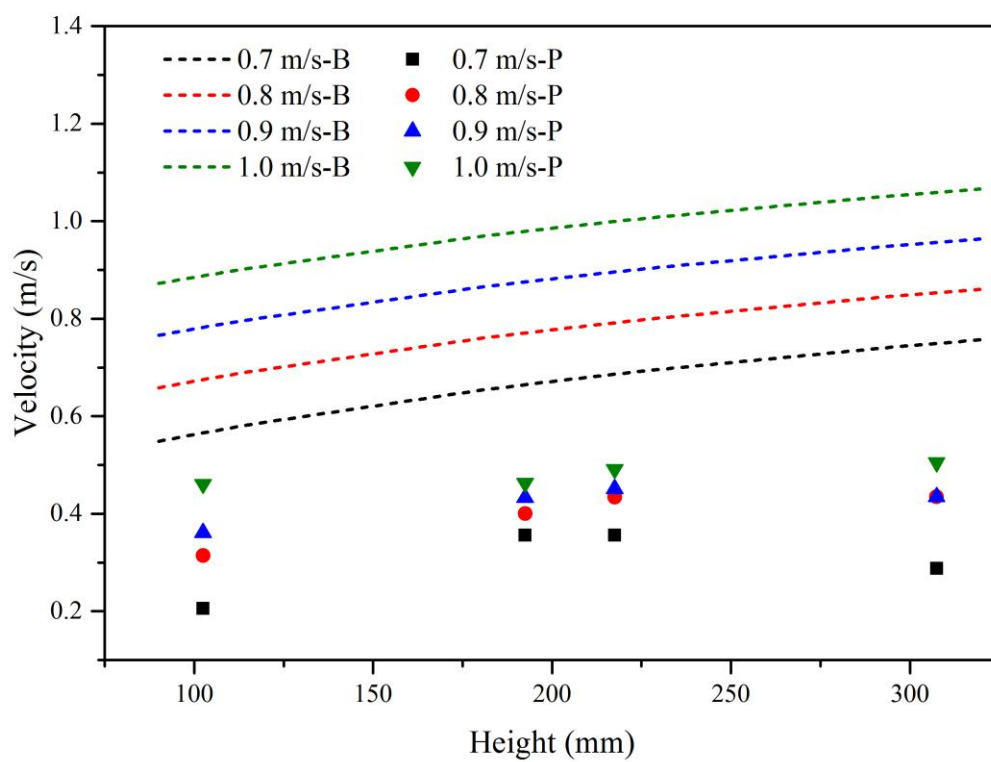


Fig. 14

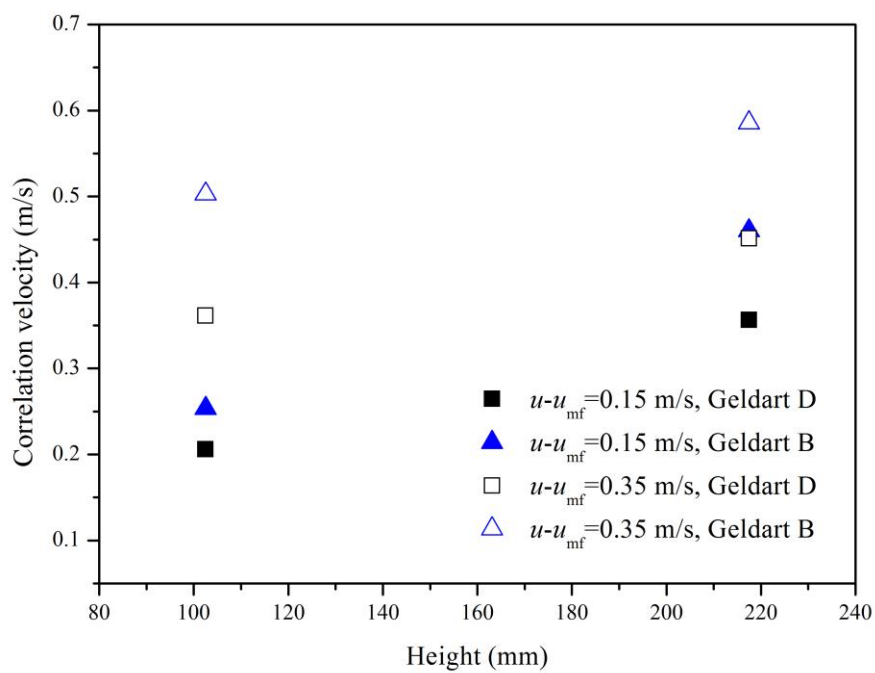


Fig. 15

ACCEPTED

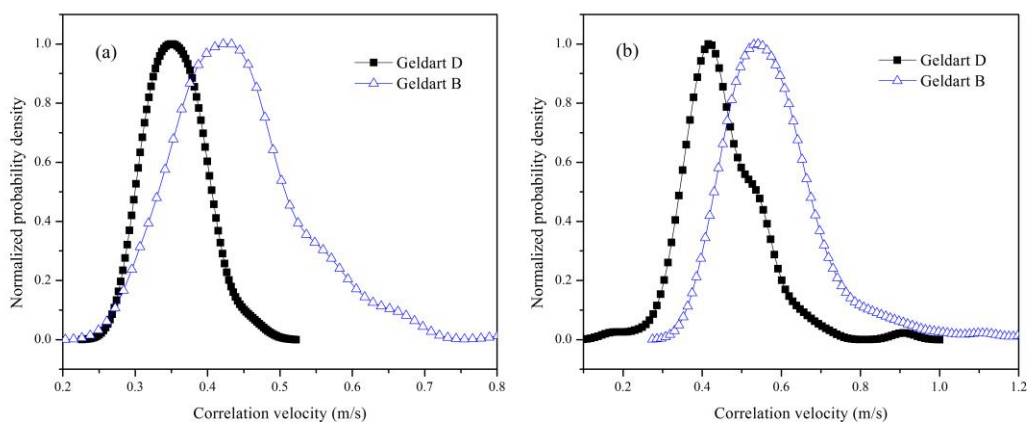


Fig. 16

Table 1. Physical properties of particles and specific operating parameters in this work

Materials	Density(kg/m ³)	Diameter (mm)	Geldart type	u_{mf} (m/s)	u (m/s)
LLDPE	918	0.45-0.90	B	0.20	0.35,0.4,0.5,0.55,0.6,0.7
PP	900	~1.85	D	0.55	0.7,0.8,0.9,1.0

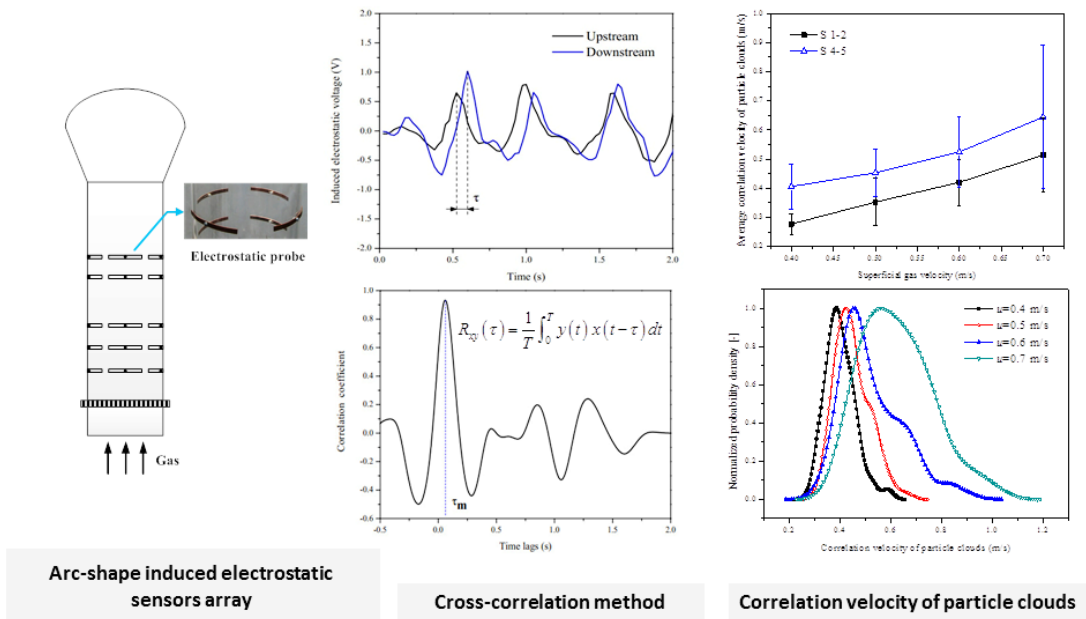
Table 2. Measurement results of average correlation velocities in the dense-phase region.

u , m/s	S 1-2		S 3-4		S 4-5		S 6-7	
	Average, m/s	STD, m/s	Average, m/s	STD, m/s	Average, m/s	STD, m/s	Average, m/s	STD, m/s
0.4	0.288	0.0125	0.389	0.0130	0.401	0.0374	0.314	0.0400
0.5	0.345	0.0148	0.452	0.0268	0.449	0.0384	0.404	0.0424
0.6	0.421	0.0179	0.521	0.0426	0.525	0.0521	0.524	0.0512
0.7	0.524	0.0128	0.555	0.0628	0.597	0.0619	0.538	0.0624

Table 3. Dynamic bed level ranges under different superficial gas velocities.

Superficial gas velocity (m/s)	0.4	0.5	0.6	0.7
Bed level range (mm)	330-410	340-440	370-520	390-590

ACCEPTED MANUSCRIPT



Graphical abstract

Highlights

- ✧ Correlation velocity of fluidized particles was measured by electrostatic sensors.
- ✧ Both upward and downward correlation velocities were measured in bed level region.
- ✧ Differences between B and D particles can be distinguished by correlation velocity.

ACCEPTED MANUSCRIPT